

Research Article

Effects of Mineral Admixtures on Macrocell Corrosion Behaviors of Steel Bars in Chloride-Contaminated Concrete

Zhong-lu Cao ^{1,2}, Zhong-chun Su ², Makoto Hibino ³, and Hiroki Goda ³

¹CCCC First Harbor Engineering Co. Ltd., Tianjin 300461, China

²CCCC Tianjin Port Engineering Institute Co. Ltd., Tianjin 300222, China

³Concrete Laboratory, Department of Civil Engineering, Kyushu Institute of Technology, Kitakyushu-shi 804-8550, Japan

Correspondence should be addressed to Zhong-lu Cao; caozhonglu@126.com

Received 1 July 2022; Accepted 2 August 2022; Published 17 August 2022

Academic Editor: Senthil Kumaran Selvaraj

Copyright © 2022 Zhong-lu Cao et al. This is an open access article distributed under the Creative Commons Attribution License, which permits unrestricted use, distribution, and reproduction in any medium, provided the original work is properly cited.

Based on the macrocell corrosion theory and by alternating the microcell corrosion state and macrocell corrosion state, the influence of mineral admixtures, such as fly ash, slag, and limestone powder, on the macrocell corrosion behaviors of steel bars embedded in chloride-contaminated concrete were investigated and clarified. The results indicated that the inhibition effect induced by slag on macrocell corrosion and microcell corrosion was obviously better than that induced by fly ash or limestone powder. The presence of slag in chloride-contaminated concrete could remarkably decrease the corrosion area ratios of anodic steel, even if the replacement levels of slag to cement reached 70%. With the addition of mineral admixtures into concrete, the ratio of macrocell current density to microcell current density was decreased to some extent, depending on the types, replacement levels, and replacement ways of mineral admixtures. The use of slag and fly ash in chloride-contaminated concrete can effectively weaken the macrocell corrosion and make the corrosion be dominated by microcell corrosion. The types and replacement levels of mineral admixtures also had a remarkable influence on the control mode of macrocell corrosion. The use of slag was more effective than that of fly ash or limestone to weaken the cathode control mode of macrocell corrosion and made the control mode of macrocell corrosion be dominated by jointed control.

1. Introduction

For marine or offshore reinforced concrete structures, such as coastal ports, cross-sea bridges, and tunnels, the durability problems caused by chloride-induced steel corrosion have always been a hot topic for engineers and scholars. There is general agreement that the most effective improvements in corrosion durability of marine reinforced concrete structures can be achieved at material selection and design stage by using mineral admixtures such as fly ash, granulated blast furnace slag, silica fume, and limestone. These mineral admixtures have been widely used in marine concrete structure to improve and enhance the corrosion durability by increasing chloride binding capacity [1–3], decreasing chloride penetration and diffusion [4], elevating chloride threshold level [5], and improving the size, shape, distribution, and structure of pores in concrete [6].

The effectiveness of mineral admixtures to inhibit the corrosion of reinforcing steel is commonly qualitatively evaluated by half-cell potential described in ASTM C876 and/or quantitatively analyzed by corrosion rate obtained from the Stern-Geary equation. The use of half-cell potential and corrosion rate is usually based on the assumption that corrosion of reinforcing steel in concrete structure is uniform, which is practicable and feasible in microcell corrosion state that the anodic zones and the cathodic zones are microscopic in sizes and located adjacent to each other. However, due to the difference of exposed environments and the heterogeneity of concrete materials, the corrosion of reinforcing steel in actually existing marine concrete structure is usually nonuniform, in that the anodic zones are far away from and separate with the cathodic zones, which leads to the formation of macrocell corrosion. When macrocell corrosion is formed, the electrochemical parameters of reinforcing steel

in cathodic zones and anodic zones could be changed under the action of macrocell potential difference, so the use of half-cell potential and corrosion rate to evaluate and judge the corrosion degree of reinforcing steel in concrete structure subjected to macrocell corrosion would not be reliable and accurate. Therefore, it is necessary to analyze and verify whether the mineral admixtures are effective or not, to improve and inhibit the macrocell corrosion of reinforcing steel in chloride-contaminated concrete.

It is well known that the types, structural compositions, chemical activities, and mixed contents of mineral admixtures could affect the anticorrosion properties of reinforcing steel. Since the microcell corrosion and macrocell corrosion are common existence in marine concrete structures, the true corrosion rate of reinforcing steel is equal to the sum of microcell corrosion rate and macrocell corrosion rate. So whether the different mineral admixtures play a different role in effecting the magnitudes of microcell corrosion and macrocell corrosion, or whether the proportional relationship between microcell corrosion and macrocell corrosion is affected by the type and mixed content of mineral admixtures, is a question worthy of consideration and attracts the interests of the authors, and as far as the authors have known, no literature gives the answer.

Additionally, known from the previous studies [7–10], the macrocell corrosion rate and control mode are mainly determined by half-cell potential and microcell current density of cathodic and anodic steels, macrocell potential difference between cathodic and anodic steels, macrocell polarization slopes, and macrocell polarization ratios of cathodic and anodic steels. The use of mineral admixtures in marine reinforced concrete structure would have an effect on these above parameters. The mechanism and efficiencies of various mineral admixtures to inhibit the macrocell corrosion have not been analyzed and compared based on these parameters mentioned above. And up to now, the effect of mineral admixtures on the control mode of macrocell corrosion is still an unknown question that attracts the interest of the authors.

For all these above reasons, in this paper, experiments were designed and carried out to investigate and clarify the effect of mineral admixtures, such as fly ash, slag, and limestone powder, on the macrocell corrosion behaviors of reinforcing steels embedded in chloride-contaminated concrete. Based on the macrocell corrosion theory and by alternating the microcell corrosion state and macrocell corrosion state, the influence of fly ash, slag, and limestone powder on the macrocell corrosion potential difference, macrocell corrosion current density, and macrocell polarization ratios of reinforcing steels was analyzed and compared, the effect of fly ash, slag, and limestone on the control mode of macrocell corrosion was clarified, and the influence of fly ash, slag, and limestone on the proportional relationships between microcell corrosion current density and macrocell corrosion current density was discussed.

2. Experiment

2.1. Materials. Hot-rolled plain steel bars with 19 mm in diameter and 180 mm in length were selected and used,

which were firstly polished by sandpaper and cleaned with acetone and then were connected to a lead wire. In order to prevent the corrosion occurring at the end of steel bar and ensure the reliability and accuracy of experimental results, the two bare ends with 40 mm in length of steel bars were coated with polystyrene resin and epoxy resin in turn. The polished surface was used to ensure that the tested steels have the same initiate surface condition. Due to the fact that the various steel surface conditions have an effect on the macrocell corrosion behaviors of steel bars [11], the seawater prerusted surface covered by black oxides with a density of 42.0 mg/cm^2 was also used to investigate the comprehensive effect of rust and mineral admixtures on the macrocell corrosion of steels.

Steel bar was centrally located in cement mortar block with a dimension of $80 \times 80 \times 160 \text{ mm}$. The mix proportion of water, binder (cement+mineral admixture), and sand in the cement mortar block was 0.6, 1.0, and 3.0. Ordinary Portland cement P.O 42.5 was used, which had a density of 3.10 g/cm^3 and met the standard requirements of GB 175. Grade II river sand that passed through the 4.75 mm opening sieve and met the specification requirements of GB/T14648 was selected as the fine aggregate, which had a density of 2.58 g/cm^3 . Mineral admixtures including grade I fly ash that met the specification requirements of GB/T1596, grade S95 slag that met the specification requirements of GB/T18046, and limestone powder that met the specification requirements of JGJ/T318 were used to replace the cement or sand in equal weight, for the purpose of investigating the influence of types, replacement levels, and replacement ways of mineral admixtures on the macrocell corrosion behaviors of reinforcing steel.

It is a slow process that chloride ions penetrate and diffuse from outer environments into the surface of steel and initiate the corrosion of steel embedded in marine concrete structures. In order to accelerate the corrosion of steel, chloride ions (3 wt% of binder) were directly added into the cement mortar at the time of casting by ways of dissolving NaCl in the mix water. Although adding chloride ions into the cement mortar made the steels have no time to be passivated and had an influence on the physical and mechanical properties of cement mortar, the reasons for doing this were firstly to accelerate the corrosion of steel, secondly to produce the same total chloride content at the steel-mortar interface transition zone, and to easily compare the effect of various mineral admixtures on the macrocell corrosion behavior of steels.

All the cement mortar blocks containing steels were allowed to set and harden in the mold for 1 day, then demolded, and continuously cured in water for the next two weeks. After that, they were allowed to dry in a laboratory environment with 20°C constant temperature for another two weeks, prior to the beginning of experiment measurements.

2.2. Methods. Experiments were designed and carried out as shown in Table 1 and Figure 1. Each case given in Table 1 consisted of two separate mortar blocks that were defined as A-side and B-side. The mortar blocks in A-side and B-

TABLE 1: Case design for the effect of various mineral admixtures.

Case no.	Cathode no.	Cathode in A-side			Anode no.	Anode in B-side			Type and levels of mineral admixture
		Initial surface state of steel bars	w/c ratio	Cl ⁻ content, wt.% of binder		Initial surface state of steel bars	w/c ratio	Cl ⁻ content, wt.% of binder	
Case 1	P60-0-5	Polished	0.60	0	P60-3-3	Polished	0.60	3	/
Case 2	P60-0-6	Polished	0.60	0	R60-3-0	Rusted by seawater	0.60	3	/
Case 3	P60-0-7	Polished	0.60	0	P60-3-L30%S	Polished	0.60	3	L30%S
Case 4	P60-0-8	Polished	0.60	0	P60-3-L15%S	Polished	0.60	3	L15%S
Case 5	P60-0-9	Polished	0.60	0	P60-3-L25%C	Polished	0.60	3	L25%C
Case 6	P60-0-10	Polished	0.60	0	P60-3-L50%C	Polished	0.60	3	L50%C
Case 7	P60-0-11	Polished	0.60	0	P60-3-L70%C	Polished	0.60	3	L70%C
Case 8	P60-0-12	Polished	0.60	0	R60-3-L70%C	Rusted by seawater	0.60	3	L70%C
Case 9	P60-0-13	Polished	0.60	0	P60-3-FA30%S	Polished	0.60	3	FA30%S
Case 10	P60-0-14	Polished	0.60	0	P60-3-FA15%S	Polished	0.60	3	FA15%S
Case 11	P60-0-15	Polished	0.60	0	P60-3-FA25%C	Polished	0.60	3	FA25%C
Case 12	P60-0-16	Polished	0.60	0	P60-3-FA50%C	Polished	0.60	3	FA50%C
Case 13	P60-0-17	Polished	0.60	0	P60-3-FA70%C	Polished	0.60	3	FA70%C
Case 14	P60-0-18	Polished	0.60	0	R60-3-FA70%C	Rusted by seawater	0.60	3	FA70%C
Case 15	P60-0-19	Polished	0.60	0	P60-3-GGB30%S	Polished	0.60	3	GGB30%S
Case 16	P60-0-20	Polished	0.60	0	P60-3-GGB15%S	Polished	0.60	3	GGB15%S
Case 17	P60-0-21	Polished	0.60	0	P60-3-GGB25%C	Polished	0.60	3	GGB25%C
Case 18	P60-0-22	Polished	0.60	0	P60-3-GGB50%C	Polished	0.60	3	GGB50%C
Case 19	P60-0-23	Polished	0.60	0	P60-3-GGB70%C	Polished	0.60	3	GGB70%C
Case 20	P60-0-24	Polished	0.60	0	R60-3-GGB70%C	Rusted by seawater	0.60	3	GGB70%C

Note: in this table, the steel bars with polished surface were marked as P, while the steel bars with the seawater prerusted surface were marked as R. Limestone powder was marked as L, fly ash was marked as FA, slag was marked as GGB, sand was marked as S, and cement was marked as C.

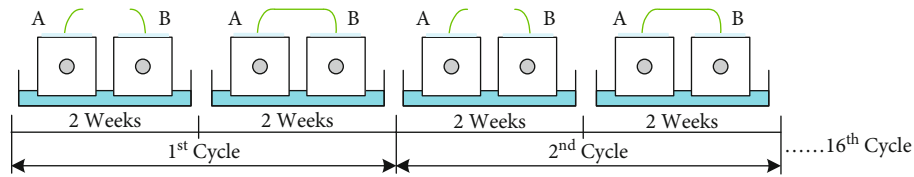


FIGURE 1: Experimental process.

side had the same water-binder ratio but contained different chloride contents and different mineral admixtures. The chloride content in the mortar blocks of A-side was 0 wt% of binder while the chloride content in the mortar blocks of B-side was 3 wt% of binder which was much higher than the chloride threshold level for active corrosion. The difference in chloride contents could form a significant half-cell potential difference between the steels in mortar blocks of A-side and B-side, which provided conditions for the formation of macrocell corrosion. Since the area ratio of cathode to anode has a remarkable influence on the macrocell corrosion current, macrocell polarization ratios, and control mode, the effect of mineral admixtures on macrocell corrosion behavior of steels would be investigated and analyzed under the condition that the area ratio of cathode to anode steel bar is 1 : 1.

In order to investigate the effect of mineral admixtures on macrocell corrosion, the mortar blocks in A-side contained 0% mineral admixture, while the mortar blocks in B-side were mixed with various mineral admixtures. For mortar blocks in B-side, mineral admixtures with various chemical activities such as fly ash, slag, and limestone powder were used to replace 25%, 50%, and 70% cement in equal weight or to replace 15% and 30% sand in equal weight, respectively. The high replacement levels of fly ash, slag, and limestone were used for the purpose of forming a notable difference in steel corrosion and allowed for clear observation of macrocell corrosion and polarization behaviors of steels. Mineral admixtures are commonly used to replace cement and rarely used to replace sand or fine aggregate. Using mineral admixtures instead of natural sand as fine aggregate of concrete can not only broaden the utilization ways of mineral admixtures but also reduce the consumption of natural sand by concrete and protect the limited natural sand resources. In literature [12], a research had been made to study the physical properties of concrete prepared by substituting a large quantity of mineral powder including fly ash, slag, and limestone for part of fine aggregate, as an alternative to Portland cement for the reduction of the environmental load, preservation of resources, and improvement of performance. Literature [13, 14] preliminary investigated the effect of nonground-granulated blast-furnace slag and bottom ash used as fine aggregate on the strengths, chloride permeability, water absorption, and freezing-thawing resistance of concrete and concluded that the slag and bottom ash can be used to replace sand or fine aggregate to produce durable concrete. Therefore, in order to broaden the usage forms and levels of mineral admixtures and reduce the consumption of natural sand by concrete, this paper attempts to clarify the influence of replacement ways and replacement

levels of limestone powder, fly ash, and slag on the microcell and macrocell corrosion durability of steel bars embedded in chloride-contaminated concrete, which would provide a solution or a suggestion for the comprehensive utilization of mineral admixtures.

The experimental process is presented in Figure 1. The steel in the mortar block of A-side acted as a cathode while the steel in the mortar block of B-side acted as an anode, which were firstly disconnected for two weeks to simulate the microcell corrosion state and then were connected for another two weeks to simulate the macrocell corrosion state. These four weeks were defined as one cycle, and 16 cycles were carried out in this study. A two-week duration was selected for both disconnected and connected periods, because it was a sufficient amount of time for the recovery and stabilization of steel corrosion state during the disconnected period and was also suitable for the stabilization of macrocell current and macrocell polarization during the connected period. The advantage of using two separate mortar blocks was that firstly, in the disconnected state, the microcell corrosion behavior of steels in A-side and B-side did not interfere with each other; secondly, in the connected state, the macrocell corrosion polarization behavior of steels in A-side and B-side could be easy to observe and investigate; and thirdly, the influence of various mineral admixtures on the proportional relationship between microcell corrosion current density and macrocell corrosion current density could be quantitatively analyzed and evaluated.

In the experimental process, mortar blocks in A-side and B-side were partially immersed in water to enhance the electroconductivity of mortar [7–11], the half-cell potential (E_{corr}) referred to the Ag/AgCl electrode, and the resistance of steel (R_p) and resistance of mortar (R_{con}) were measured at set intervals by the use of a corrosion detection device CM-SE1 developed by Nippon Steel Techno Research. Microcell corrosion current density of steel was defined as the corrosion current density of steel in the disconnected periods [15–18], which was calculated by the use of the Stern-Geary equation: $i_{\text{corr-mi}} = B/R_p$, where R_p was the resistance of steel and B was a constant which was commonly considered to be 26 mV for steel in a corroded state and 52 mV for steel in a passive state. Macrocell corrosion current density of steel was calculated by the equation: $i_{\text{corr-ma}} = I_{\text{ma}}/A_a$, where I_{ma} was the macrocell current flowing between cathode (steel in A-side) and anode (steel in B-side) and A_a was the surface area of steel that acted as an anode. In the connected periods, macrocell current naturally flowing between A-side and B-side was directly measured by zero resistance ammeters.

The effect of mineral admixtures on the macrocell corrosion behaviors of steels was also analyzed and evaluated by the use of macrocell potential difference, macrocell polarization ratios, and macrocell corrosion control mode. The definition and calculation of these parameters were given in literatures [7–9]. Macrocell potential difference $\Delta E_{\text{corr}1}$ was defined as the potential difference between the cathode and anode during the disconnected periods, and $\Delta E_{\text{corr}4}$ was the potential difference between the cathode and anode during the connected periods. While $\Delta E_{\text{corr}2}$ was the potential difference of cathodic steel during the disconnected periods and connected periods, $\Delta E_{\text{corr}3}$ was the potential difference of anodic steel during the disconnected periods and connected periods. In the macrocell corrosion state, it was important to know the relative contributions from the polarization of the cathode and anode and the mortar resistance, as described by $\Delta E_{\text{corr}1} = \Delta E_{\text{corr}2} + \Delta E_{\text{corr}3} + \Delta E_{\text{corr}4}$, or in another way, $1 = \Delta E_{\text{corr}2}/\Delta E_{\text{corr}1} + \Delta E_{\text{corr}3}/\Delta E_{\text{corr}1} + \Delta E_{\text{corr}4}/\Delta E_{\text{corr}1}$, which had been graphically illustrated in literatures [7–9]. The ratios of $\Delta E_{\text{corr}2}/\Delta E_{\text{corr}1}$, $\Delta E_{\text{corr}3}/\Delta E_{\text{corr}1}$, and $\Delta E_{\text{corr}4}/\Delta E_{\text{corr}1}$ were defined as the macrocell polarization ratio of the cathode, the macrocell polarization ratio of the anode, and the macrocell polarization ratio of mortar resistance, respectively.

3. Results and Discussions

3.1. Time Evolution Curves of Corrosion Parameters. Due to the difference of particle size, chemical compositions, and hydration activity, the usage of limestone powder, fly ash, and slag in concrete would inevitably have an impact on concrete microstructure, porosity, pore solution chemistry, and chloride binding capacity [1, 6, 12, 19, 20] and then affect the availability of oxygen, internal humidity, and concrete resistivity. The changes of concrete internal environments, such as oxygen, humidity, and resistivity, induced by the use of mineral admixtures, would have a direct impact on the corrosion behaviors of steel bars, which could be reflected by the changes of corrosion parameters such as half-cell potential, microcell corrosion current density, and macrocell corrosion current density.

Because the time evolution curves of corrosion parameters such as half-cell potential, microcell corrosion current density, macrocell corrosion current density, and mortar resistance for all cases designed in Table 1 had the same expression way, only the results of case 1, case 5, case 11, and case 17 were given out and are shown in Figure 2. It can be seen from these figures, in the disconnected state, there was a remarkable difference in half-cell potential, microcell corrosion current density, and mortar resistance between the cathode (specimen in A-side) and anode (specimen in B-side), which created the condition for the formation of macrocell corrosion. When the cathodic steel of A-side was connected with the anodic steel of B-side, macrocell corrosion was formed, and the macrocell polarization behaviors of cathodic steel and anodic steel were clearly observed. Under the action of electrochemical driving force in terms of macrocell potential difference, the half-cell potential of cathodic steel was polarized to a lower value while the

half-cell potential of anodic steel was polarized to a higher value. The electrons released by the anodic steel of B-side were partly transferred to and consumed by the cathodic steel of A-side, which resulted in the flow of macrocell current from the cathode to anode.

For all cases designed in Table 1, the compositions, materials, and experimental conditions of cathode (specimen in A-side) were the same, so the ability of cathodic steels in A-side to consume and react with the electrons was considered to be the same and keep the relative constant during the whole experimental process. Therefore, the macrocell current flowing between the cathode and anode was mainly controlled by the ability of anodic steel in B-side to release the electrons. The change of types, replacement levels, and replacement ways of mineral admixtures could have an effect on the moisture content of mortar, the diffusion and transmission of oxygen, the chloride binding capacity, the change of microstructure in the interface transition zone between steel and mortar, and the change of composition of iron oxides formed on the steel surface and therefore could have a direct influence on the ability of anodic steels to release electrons and finally affect the magnitude of macrocell potential difference and the magnitude of macrocell current density, as well as the macrocell polarization ratio and the control mode of macrocell corrosion.

3.2. Effect of Mineral Admixtures on the Macrocell Potential Difference and Macrocell Current Density. The effect of replacement levels and replacement ways of limestone powder, fly ash, and slag on the macrocell potential difference and macrocell current density is presented in Figure 3. The use of mineral admixtures to replace sand with the same amount was more effective than that to replace cement, to reduce both the macrocell potential difference and macrocell current density. When mineral admixtures were used to replace cement with the same amount, the macrocell potential difference $\Delta E_{\text{corr}1}$ increased gradually with the increasing replacement levels, while the macrocell current density decreased firstly and then increased. The macrocell current density is the minimum at the 25% replacement level of mineral admixtures to cement. When limestone powder, fly ash, and slag had the same replacement levels, the inhibition effect induced by slag on macrocell corrosion was obviously better than that induced by fly ash or limestone powder.

At the conditions that no mineral admixtures were used, such as case 1 and case 2, the initiate prerusted surface of steel was helpful in reducing the macrocell current density and weakening the macrocell corrosion. However, when the replacement levels of limestone powder, fly ash, and slag were higher and reached to 70%, such as case 8, case 14, and case 20, the initiate prerusted surface of steel could result in the increase in macrocell current density and accelerate the macrocell corrosion.

3.3. Effect of Mineral Admixtures on the Relationship between Microcell Current Density and Macrocell Current Density. As shown in Figure 4, using limestone powder, fly ash, or slag to replace sand was more effective than that to replace cement,

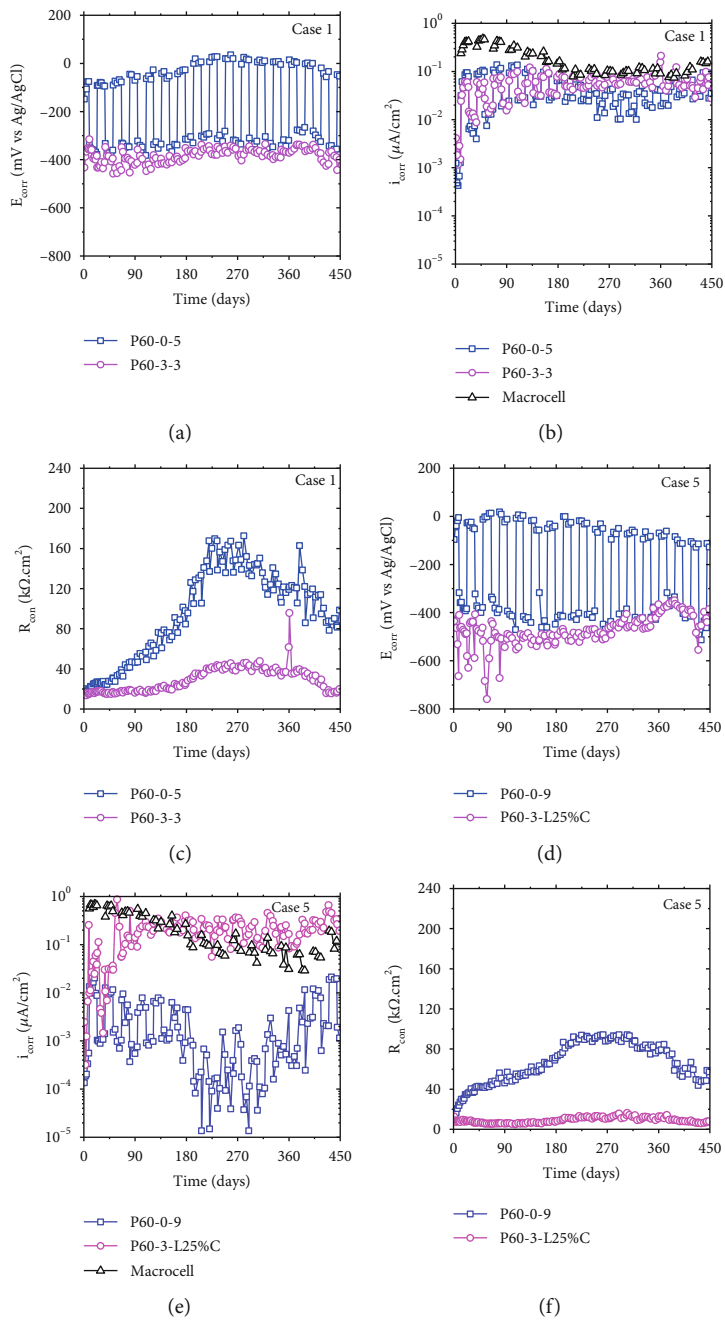


FIGURE 2: Continued.

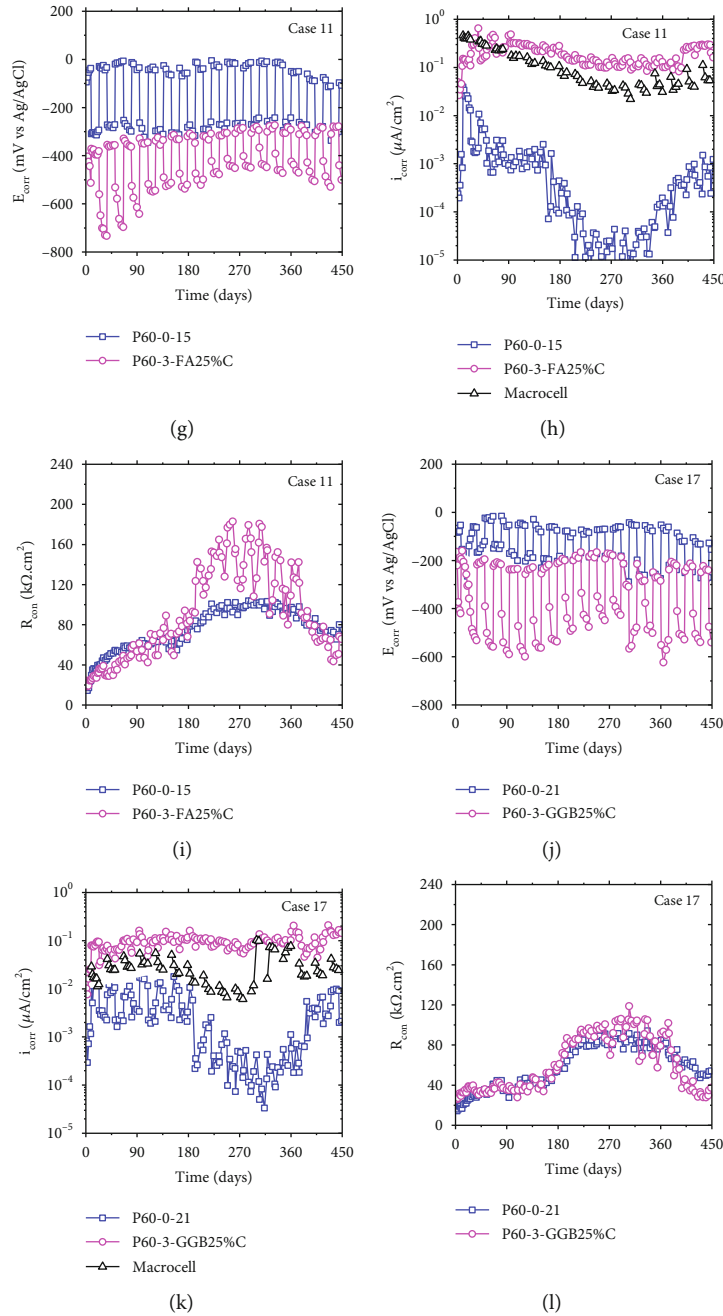


FIGURE 2: Time evolution curves of corrosion parameters such as half-cell potential, microcell corrosion current density, macrocell corrosion current density, and mortar resistance for case 1, case 5, case 11, and case 17: (a) half-cell potential of steel in case 1, (b) corrosion current density of steel in case 1, (c) resistance of the mortar in case 1, (d) half-cell potential of steel in case 5, (e) corrosion current density of steel in case 5, (f) resistance of the mortar in case 5, (g) half-cell potential of steel in case 11, (h) corrosion current density of steel in case 11, (i) resistance of the mortar in case 11, (j) half-cell potential of steel in case 17, (k) corrosion current density of steel in case 17, and (l) resistance of the mortar in case 17.

to reduce both the microcell current density and macrocell current density. The higher the replacement levels of mineral admixtures to sand, the more obvious the decrease in microcell current density and macrocell current density. When limestone, fly ash, or slag was used to replace cement, there was an optimal replacement level to minimize the macrocell current density, but it could not effectively reduce the microcell current density. The higher replacement levels of min-

eral admixtures to cement had a risk of increasing the microcell current density. When the replacement levels of limestone, fly ash, and slag were constant, the inhibition effect induced by slag on the microcell and macrocell current density was obviously better than that induced by fly ash or limestone. Whether mineral admixtures, such as limestone, fly ash, and slag, were added or not, the initiate prerusted surface of steel was less helpful in reducing the microcell

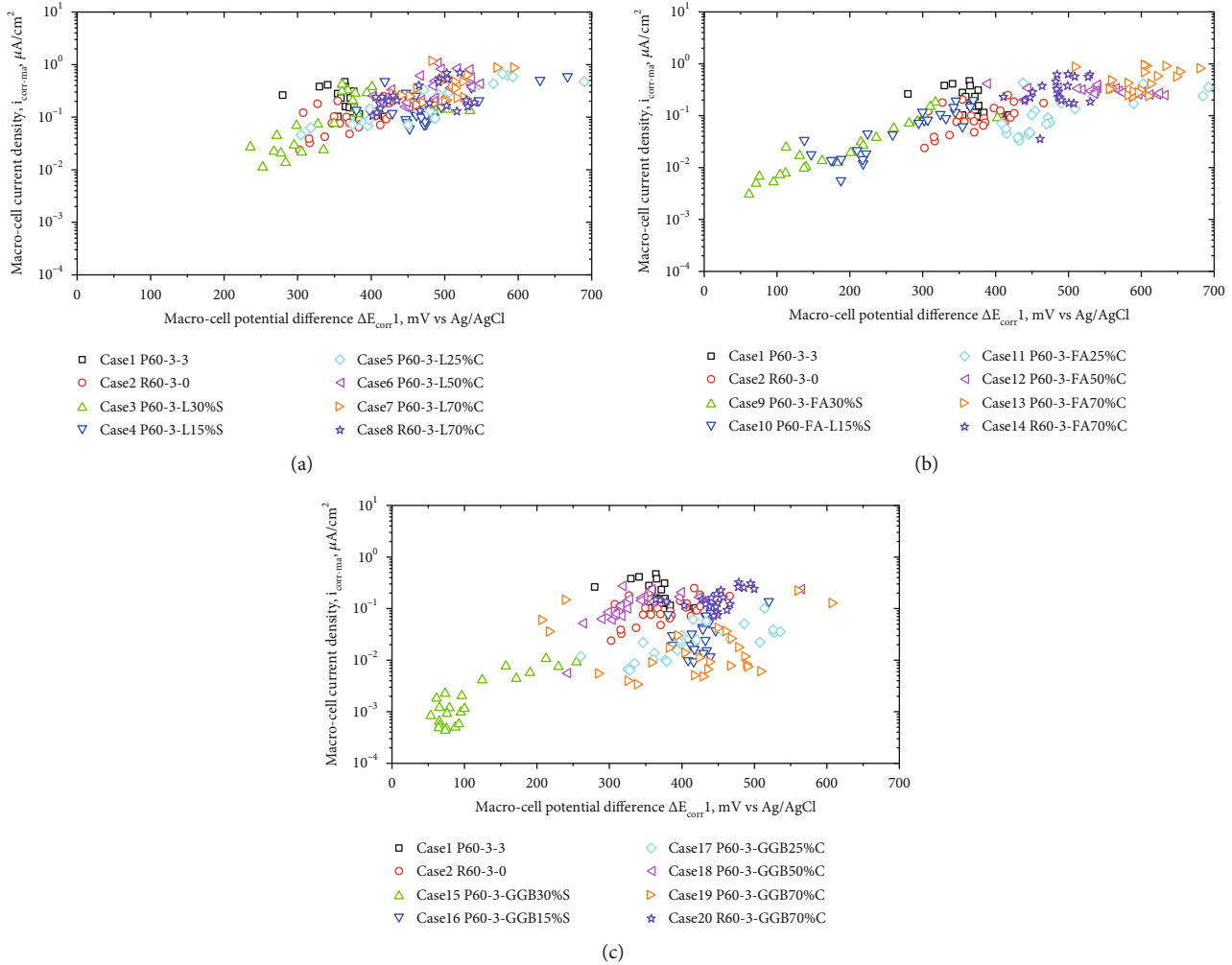


FIGURE 3: Effect of the replacement levels of (a) limestone, (b) fly ash, and (c) slag on the relationships between $\Delta E_{\text{corr}1}$ and macrocell current density.

current density. The presence of initiate prerusted surface could accelerate the microcell corrosion of steel.

With the addition of mineral admixtures into concrete, the ratio of macrocell current density to microcell current density was decreased to some extent, depending on the types, replacement levels, and replacement ways of mineral admixtures. The use of mineral admixtures, especially slag and fly ash in chloride-contaminated concrete, can effectively weaken the macrocell corrosion and make the corrosion be dominated by microcell corrosion.

3.4. Effect of Mineral Admixtures on the Macrocell Polarization Ratios and Control Mode. The magnitude of macrocell polarization ratios of cathodic steel, anodic steel, and concrete resistance has determined the control mode of macrocell corrosion. The macrocell polarization ratios of cathodic steel and anodic steel induced by limestone powder, fly ash, and slag are given in Figures 5–7, respectively.

Whether limestone was used to replace cement or sand, the macrocell polarization ratio of cathodic steel was always greater than 0.60, and that of anodic steel was less than 0.30,

so the control mode of macrocell corrosion was always cathode control. The replacement levels and replacement ways of limestone powder had an influence on the macrocell potential difference but had little effect on the control mode of macrocell corrosion.

The use of fly ash to replace 15% and 30% sand or 50% and 70% cement had a remarkable effect on the macrocell potential difference but had less influence on the macrocell polarization ratio of cathodic steel and anodic steel, the macrocell polarization ratio of cathodic steel was always greater than 0.60, and that of anodic steel was less than 0.30; the macrocell corrosion was always in the mode of cathode control. However, when fly ash was used to replace 25% cement, the macrocell polarization ratio of cathodic steel was decreased and distributed in the range of 0.30 to 0.60, and that of anodic steel was increased and distributed in the range of 0.30 to 0.60; the macrocell corrosion was considered to be controlled by both cathodic steel and anodic steel, which was a jointed control mode.

The replacement levels of slag to sand or cement not only had a significant influence on the macrocell potential

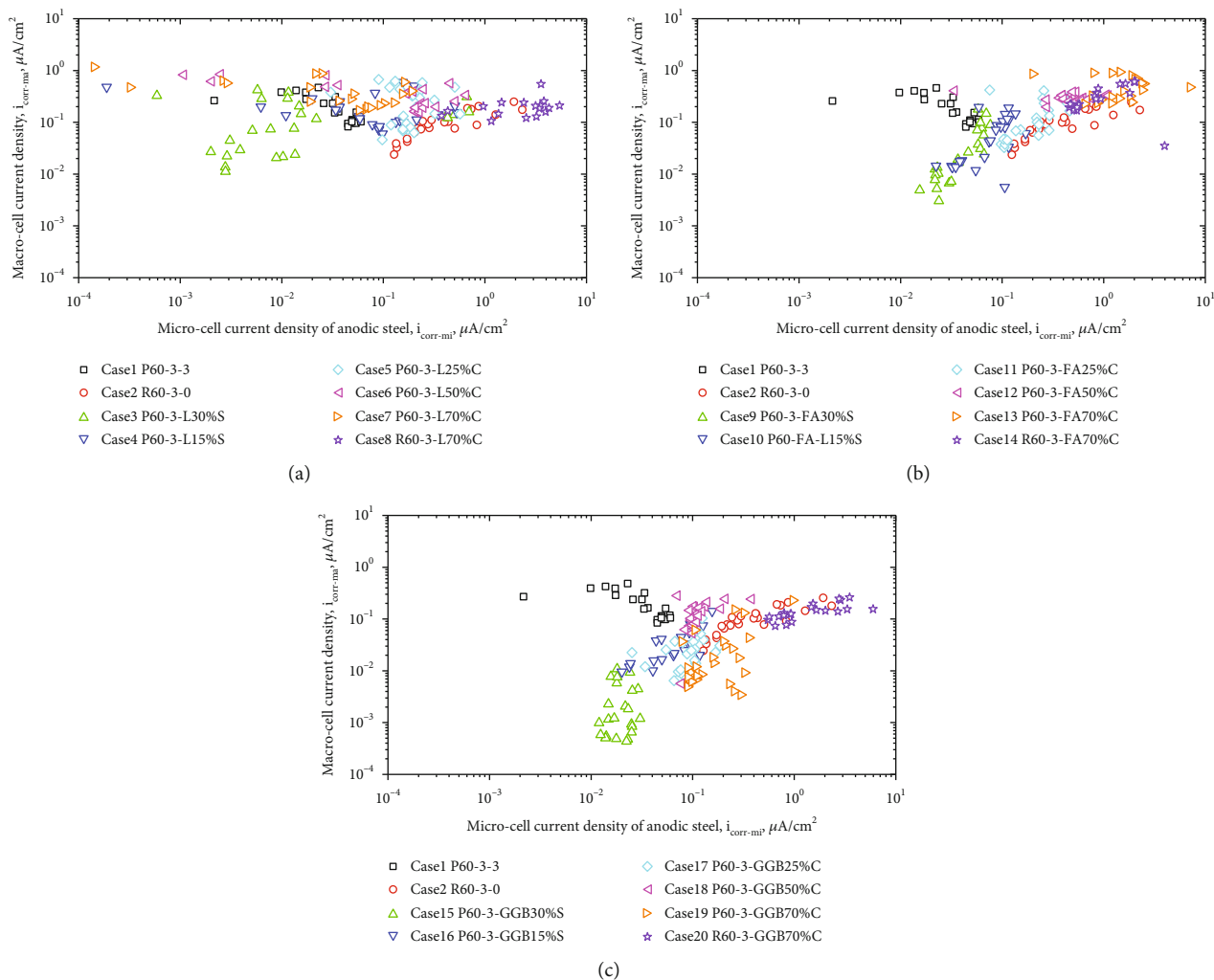


FIGURE 4: Effect of the replacement levels of (a) limestone powder, (b) fly ash, and (c) slag on the relationships between microcell current density and macrocell current density.

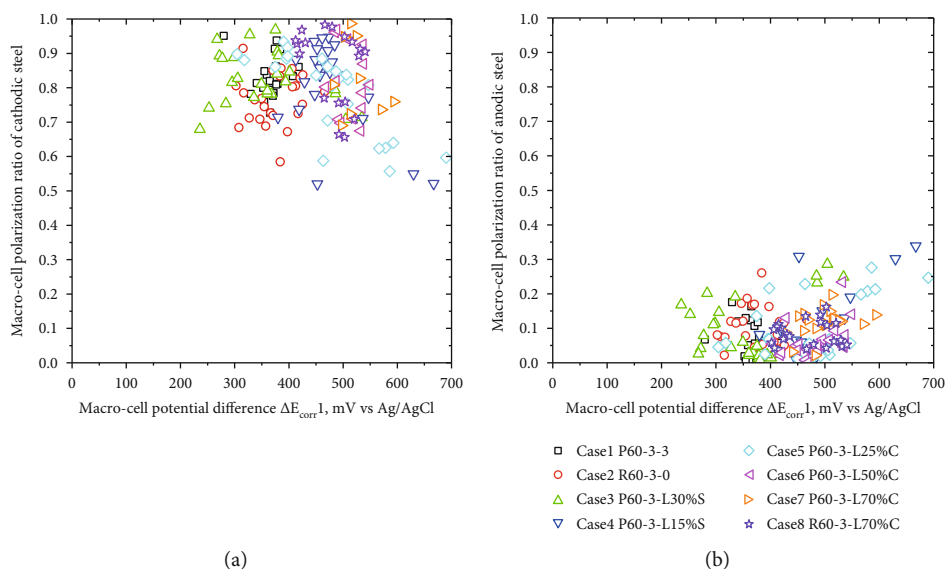


FIGURE 5: Effect of the replacement levels of limestone powder on the macrocell polarization ratios of cathodic steel and anodic steel.

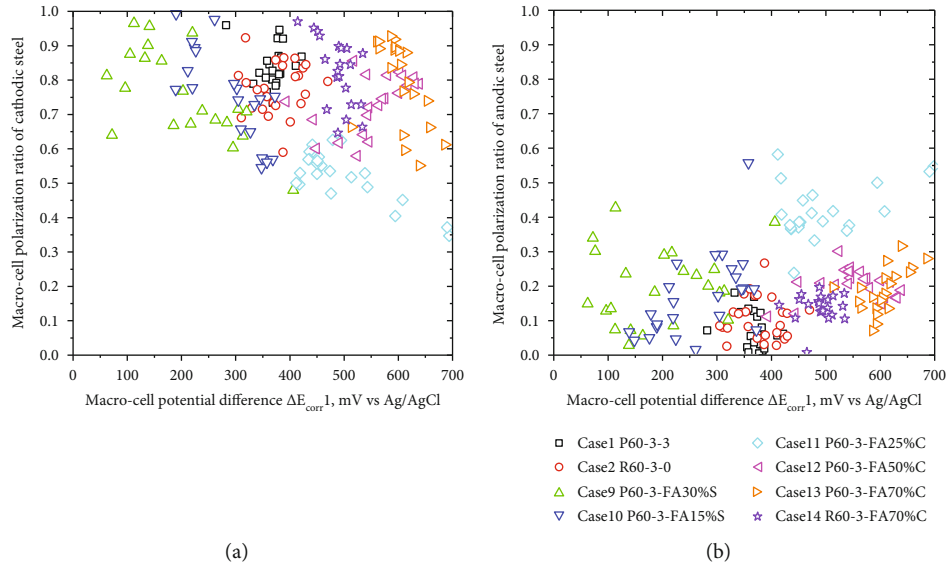


FIGURE 6: Effect of the replacement levels of fly ash on the macrocell polarization ratios of cathodic steel and anodic steel.

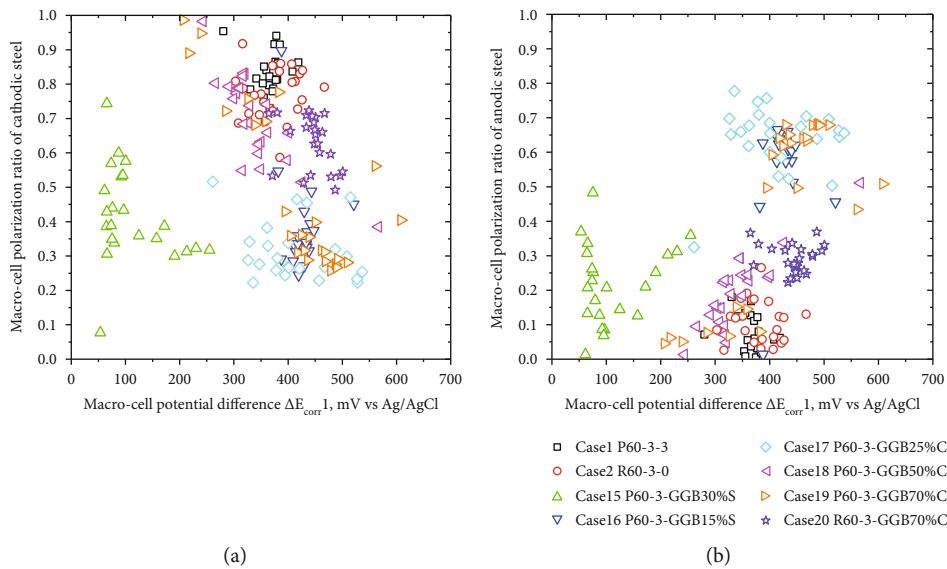


FIGURE 7: Effect of the replacement levels of slag on the macrocell polarization ratios of cathodic steel and anodic steel.

difference but also had an effect on the macrocell polarization ratio of cathodic steel and anodic steel. For case 1, the macrocell polarization ratio of cathodic steel was distributed in the range of 0.77 to 0.94, while that of anodic steel was distributed in the range of 0.01 to 0.14; the control mode of macrocell corrosion was typically cathode control. Compared with case 14, when slag was used to replace 30% sand, the macrocell polarization ratio of cathodic steel was decreased and distributed in the range of 0.30 to 0.60, and that of anodic steel was increased and distributed in the range of 0.10 to 0.36, which means that the cathode control mode was weakened and the macrocell corrosion was jointly controlled by the cathode and anode. When slag was used to replace 15% sand, the macrocell polarization ratio of

cathodic steel was further decreased and distributed in the range of 0.24 to 0.45, and that of anodic steel was further increased and distributed in the range of 0.44 to 0.66, which made the control mode of macrocell corrosion be dominated by jointed control. When slag was used to replace 25% cement, the macrocell polarization ratio of cathodic steel was distributed in the range of 0.20 to 0.40, and that of anodic steel was distributed in the range of 0.50 to 0.77; the control mode of macrocell corrosion was dominated by jointed control or by anode control. However, with the further increase in the replacement level of slag to cement, the macrocell polarization ratio of cathodic steel had a trend to increase and that of anodic steel had a trend to decrease. When slag was used to replace 50% or 70% cement, the

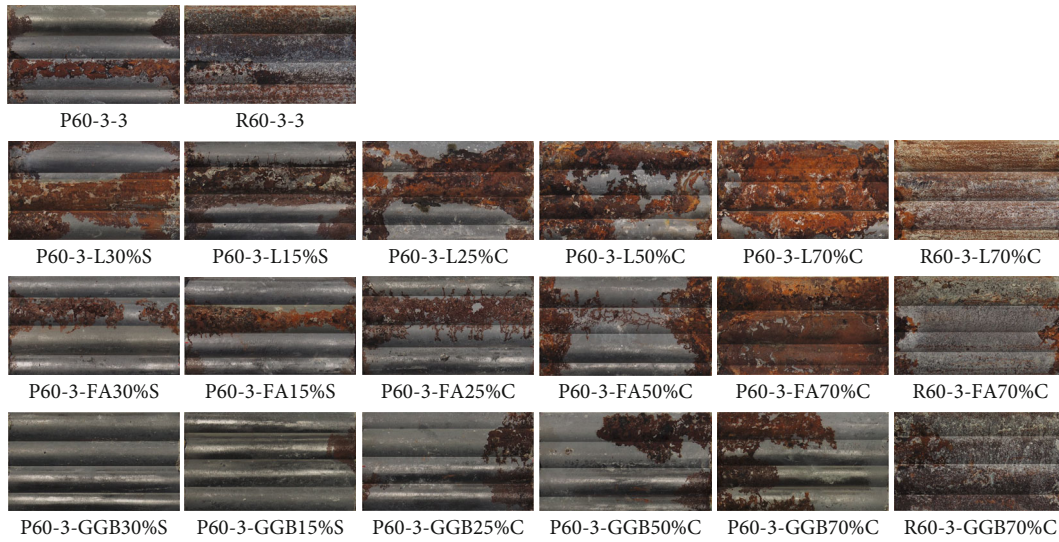


FIGURE 8: Corrosion states of anodic steel in chloride-contaminated concrete with various amounts of limestone powder, fly ash, and slag.

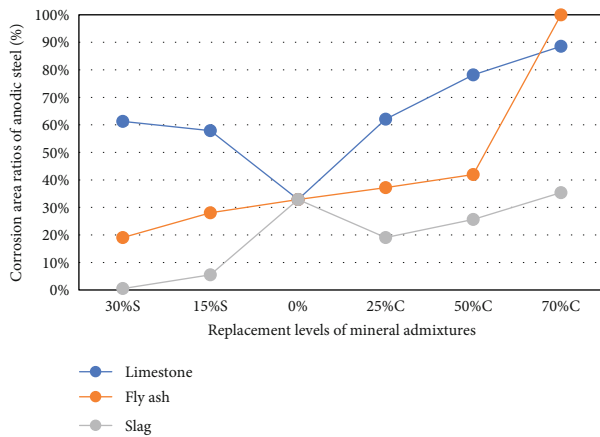


FIGURE 9: Corrosion area ratios of anodic steel in chloride-contaminated concrete with various replacement levels of mineral admixtures.

macrocell polarization ratio of cathodic steel was distributed in the range of 0.27 to 0.94, and that of anodic steel was distributed in the range of 0.04 to 0.67; the macrocell corrosion was dominated by jointed control or by cathode control.

3.5. Effect of Mineral Admixtures on the Corrosion State of Anodic Steel. In order to check the real corrosion state of anodic steel and confirm the effect of various mineral admixtures on the corrosion, at the end of experiments, mortar blocks of B-side were split and the anodic steels were taken out and observed. The true corrosion states and corrosion area ratios of anodic steel in chloride-contaminated concrete with various amounts of limestone, fly ash, and slag are presented in Figures 8 and 9.

The types and replacement levels of mineral admixtures played an important role in controlling the corrosion degree of anodic steel. For the same replacement level, slag was the most effective in inhibiting the corrosion area of anodic steel,

followed by fly ash and limestone powder. Using limestone powder to replace cement or sand could not effectively improve the corrosion area ratios of anodic steel. In particular, the presence of limestone powder in concrete to replace cement in equal weight had a risk of accelerating the corrosion of anodic steels. Using fly ash to replace sand had a positive effect on decreasing the corrosion area ratios of anodic steels, but using fly ash to replace cement could not effectively reduce the corrosion area ratios of anodic steels, especially when the replacement amount of cement was more than 50%. Due to the high activity of slag, the presence of slag in chloride-contaminated concrete could remarkably decrease the corrosion area ratios of anodic steel and significantly inhibit the corrosion of anodic steels, even if the replacement levels of slag to cement reached 70%. Compared to fly ash and limestone powder, the use of slag in concrete could not only improve the porosity of the interfacial transition zone and make it denser and have lower permeability but also enhance the chloride binding capacity [3, 6, 12, 19–21] and reduce the free chloride content and therefore weaken the function of chloride ions to induce corrosion.

4. Conclusions

The use of mineral admixtures to replace sand was more effective than that to replace cement, to reduce both the macrocell current density and microcell current density. When limestone powder, fly ash, and slag had the same replacement levels, the inhibition effect induced by slag on macrocell corrosion and microcell corrosion was obviously better than that induced by fly ash or limestone.

With the addition of mineral admixtures into concrete, the ratio of macrocell current density to microcell current density was decreased to some extent, depending on the types, replacement levels, and replacement ways of mineral admixtures. The use of mineral admixtures, especially slag and fly ash in chloride-contaminated concrete, can effectively

weaken the macrocell corrosion and make the corrosion be dominated by microcell corrosion.

The types and replacement levels of mineral admixtures had a significant effect on the macrocell polarization ratio of cathodic steel and anodic steel and therefore had a remarkable influence on the control mode of macrocell corrosion. The use of slag was more effective than that of fly ash or limestone to weaken the cathode control mode of macrocell corrosion and made the control mode of macrocell corrosion be dominated by jointed control.

Compared to fly ash and limestone powder, the presence of slag in chloride-contaminated concrete could remarkably decrease the corrosion area ratios of anodic steel, even if the replacement levels of slag to cement reached 70%.

Data Availability

The data used to support the findings of this study are available from the corresponding author upon request.

Conflicts of Interest

The authors declare that there is no conflict of interests regarding the publication of this paper.

Acknowledgments

This study was funded by the Science and Technology Research and Development Project (No. 2016-9-3) of CCCC First Harbor Engineering Co. Ltd.

References

- [1] X. Shi, N. Xie, K. Fortune, and J. Gong, "Durability of steel reinforced concrete in chloride environments: an overview," *Construction and Building Materials*, vol. 30, pp. 125–138, 2012.
- [2] T. Cheewaket, C. Jaturapitakkul, and W. Chalee, "Long term performance of chloride binding capacity in fly ash concrete in a marine environment," *Construction and Building Materials*, vol. 24, no. 8, pp. 1352–1357, 2010.
- [3] Q. Ding, J. Geng, S. Hu, J. Sun, and B. Sun, "Different effects of fly ash and slag on anti-rebar corrosion ability of concrete with chloride ion," *Wuhan University Journal of Natural Sciences*, vol. 14, no. 4, pp. 355–361, 2009.
- [4] V. M. Malhotra, M. H. Zhang, and G. H. Leaman, "Long-term performance of steel reinforcing bars in Portland cement concrete incorporating moderate and high volumes of ASTM class F fly ash," *Materials Journal*, vol. 97, no. 4, pp. 409–417, 2000.
- [5] C. Andrade and R. Buják, "Effects of some mineral additions to Portland cement on reinforcement corrosion," *Cement and Concrete Research*, vol. 53, pp. 59–67, 2013.
- [6] H. W. Song and V. Sarawathy, "Studies on the corrosion resistance of reinforced steel in concrete with ground granulated blast-furnace slag—an overview," *Journal of Hazardous Materials*, vol. 138, no. 2, pp. 226–233, 2006.
- [7] Z. Cao, M. Hibino, and H. Goda, "Effect of water-cement ratio on the macrocell polarization behavior of reinforcing steel," *Journal of Engineering*, vol. 2014, Article ID 925410, 11 pages, 2014.
- [8] Z. Cao, M. Hibino, and H. Goda, "Effect of nitrite inhibitor on the macrocell corrosion behavior of reinforcing steel," *Journal of Chemistry*, vol. 2015, Article ID 402182, 15 pages, 2015.
- [9] Z. L. Cao, H. Y. Chen, L. Y. Wei, and M. Hibino, "Effect of anodic and cathodic chloride contents on the macrocell corrosion and polarization behavior of reinforcing steel," *International Journal of Engineering Research in Africa*, vol. 22, pp. 45–58, 2016.
- [10] Z. L. Cao, "Effect of water conditions on macro-cell corrosion potential difference and current density of reinforcing steel in concrete," *Key Engineering Materials*, vol. 831, pp. 87–94, 2020.
- [11] Z. L. Cao, M. Hibino, and H. Goda, "Effect of steel surface conditions on the macro-cell polarization behavior of reinforcing steel," *Applied Mechanics and Materials*, vol. 584, pp. 1771–1779, 2014.
- [12] H. Uchikawa, S. Hanehara, and H. Hirao, "Influence of microstructure on the physical properties of concrete prepared by substituting mineral powder for part of fine aggregate," *Cement and Concrete Research*, vol. 26, no. 1, pp. 101–111, 1996.
- [13] I. Yüksel, Ö. Özkan, and T. Bilir, "Use of granulated blast-furnace slag in concrete as fine aggregate," *ACI MatSerials Journal*, vol. 103, no. 3, pp. 203–208, 2006.
- [14] İ. Yüksel, T. Bilir, and Ö. Özkan, "Durability of concrete incorporating non-ground blast furnace slag and bottom ash as fine aggregate," *Building and Environment*, vol. 42, no. 7, pp. 2651–2659, 2007.
- [15] C. M. Hansson, A. Poursae, and A. Laurent, "Macrocell and microcell corrosion of steel in ordinary Portland cement and high performance concretes," *Cement and Concrete Research*, vol. 36, no. 11, pp. 2098–2102, 2006.
- [16] A. Poursae, A. Laurent, and C. M. Hansson, "Corrosion of steel bars in OPC mortar exposed to NaCl, MgCl₂ and CaCl₂: macro- and micro-cell corrosion perspective," *Cement and Concrete Research*, vol. 40, no. 3, pp. 426–430, 2010.
- [17] T. Maruya, H. Takeda, K. Horiguchi, S. Koyama, and K. L. Hsu, "Simulation of steel corrosion in concrete based on the model of macro-cell corrosion circuit," *Journal of Advanced Concrete Technology*, vol. 5, no. 3, pp. 343–362, 2007.
- [18] C. Andrade, I. R. Maribona, S. Feliu, J. A. González, and S. Feliu Jr., "The effect of macrocells between active and passive areas of steel reinforcements," *Corrosion Science*, vol. 33, no. 2, pp. 237–249, 1992.
- [19] K. E. Hassan, J. G. Cabrera, and R. S. Maliehe, "The effect of mineral admixtures on the properties of high-performance concrete," *Cement and Concrete Composites*, vol. 22, no. 4, pp. 267–271, 2000.
- [20] F. Li, Y. Chen, S. Long, and J. Chen, "Properties and microstructure of marine concrete with composite mineral admixture," *Journal of Wuhan University of Technology-Mater.*, vol. 24, no. 3, pp. 497–501, 2009.
- [21] A. Leemann, R. Loser, and B. Münch, "Influence of cement type on ITZ porosity and chloride resistance of self-compacting concrete," *Cement and Concrete Composites*, vol. 32, no. 2, pp. 116–120, 2010.